

# A NATURAL PIXEL DECOMPOSITION FOR TOMOGRAPHIC IMAGING OF THE IONOSPHERE.

*Joshua Semeter*

Max-Planck-Institut  
für extraterrestrische Physik  
Postfach 1603  
85740 Garching

*Farzad Kamalabadi*

Department of Electrical  
and Computer Engineering  
Boston University  
725 Commonwealth Avenue  
Boston, MA 02215

## ABSTRACT

We apply a natural pixel (NP) decomposition to the problem of computerized ionospheric tomography (CIT). For tomography from very few angles, the NP approach provides some distinct advantages over standard basis expansions. The NP solution requires no prior assumption and as such embeds into the solution the natural spatial resolution supported by the data. For the uniquely constrained CIT geometry, however, NP estimated fields will contain significant negative values. We propose a method of improving the NP estimates by enforcing positivity through an entropy regularization algorithm. These techniques are demonstrated in an example.

## 1. INTRODUCTION

Space physics research relies heavily on ground-based measurements of the near-Earth plasma environment. Many of the direct parameters measured are of a line-of-site integrated nature. For example, radio techniques are routinely used to determine the total electron content (TEC) between a ground receiver and a radio beacon on a transiting satellite. Similarly, photometric brightness measurements of ionospheric optical emission (such as those occurring in the aurora-borealis) represent an integration of the total photon emission rate within a detector's field of view. Much attention has been focussed in recent years on the application of tomographic techniques to both radio [1][2] and optical [3][4] measurements. We refer to these problems collectively as *computerized ionospheric tomography* (CIT). Both give rise to a tomographic geometry shown schematically in Figure 1. For clarity, we have shown only a few lines-of-site through the region of interest  $\Omega$ . In radio tomography, these lines connect to a transiting satellite above  $\Omega$ , as indicated by the dashed

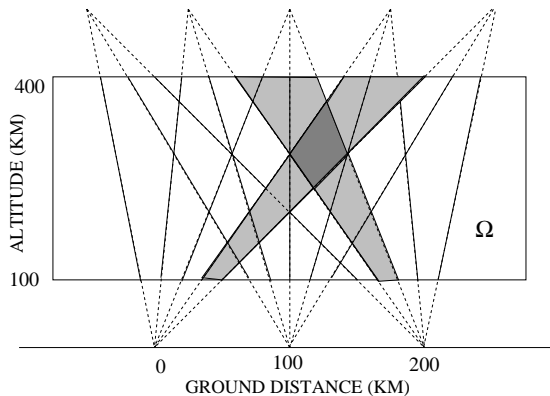


Figure 1: Schematic illustration of CIT geometry.

lines. In optical tomography, the detector elements define fan beams through  $\Omega$ .

Due to the limited angle nature of the data acquisition geometry, standard transform-based reconstruction algorithms such as filtered-back-projection (FBP) are not suitable for ionospheric tomography. Consequently, CIT relies on an algebraic formulation that generally involves a rectangular pixelization of  $\Omega$ . The extreme ill-conditioning imposed by the viewing geometry is often handled in a heuristic fashion, either with some assumption on the vertical shape [4] or by decomposing the solution onto a set of orthogonal basis functions that is assumed to span the space of feasible structures [1].

This paper instead casts ionospheric tomography in the framework of a “natural pixel” (NP) basis. The NP reconstruction makes no prior assumption on the solution, and so embeds in the solution the natural resolution supported by the data. This concept has been formalized in development of multiscale basis expansions for tomography, which develop natural from the NP approach [5]. The NP solution also operates on

a much smaller inverse problem, and is therefore useful to consider first when evaluating any limited angle tomography problem.

## 2. PRELIMINARIES

In principle, one can formulate a tomographic inversion problem whenever an unknown field can be related to a set of integrals of some property of the field. As such tomography is concerned with solutions to the Fredholm integral equation of the first kind with a square integrable kernel

$$y(\rho) = \int_a^b K(\rho, \gamma) f(\gamma) d\gamma \quad (1)$$

where  $f$  is the unknown function,  $y$  is the measurement and the kernel  $K$  is chosen with regard to the desired solution and the nature of the measurements. While the discretization of  $y$  is generally specified by the measurement process, we are free to choose  $K$ . To our knowledge, all approaches to solving the ionospheric tomographic problem have incorporated some a priori basis expansion of the object field. Appropriate lexicographic ordering leads to a sparse matrix equation of the form

$$y = Tf \quad (2)$$

where  $y$  is the vector of measurements,  $f$  is the vector of coefficients, and  $T$  is a matrix whose elements relate the measurements  $y$  to the unknown parameterized field  $f$ .

There are several unavoidable problems with this formulation. The first is that for any nontrivial discretization,  $T$  is generally ill-conditioned regardless of the number or spacing of ground stations. Among other problems, this means that the solution will generally depend on the initial guess. A second problem is that for such limited data, it is not clear what basis expansion should be chosen. One must generally rely on intuition or some physical model in parameterizing the field. A third problem is that for many bases,  $T$  is very large and sparse, leading to storage problems and great computational overhead. Moreover, the sparseness has no particularly useful structure that may be exploited. And lastly, this formulation hinders accurate representation of the physical generation of the measurements.

## 3. THE NATURAL PIXEL DECOMPOSITION

We now present an alternative basis that is closely connected with the measurement geometry. Suppose we have a total of  $N_t$  measurements from  $N_p$  observation sites. Let  $\mathbf{r}$  represent the position vector in  $\Omega$ . For

each of the  $N_t$  measurements we define a characteristic function

$$\phi_i(\mathbf{r}) = \begin{cases} 1 & \text{if } \mathbf{r} \text{ lies in the field of view of pixel } i \\ 0 & \text{otherwise} \end{cases} \quad (3)$$

The functions  $\phi_i(\mathbf{r})$  are called ‘‘the natural pixels’’, and are uniquely defined for a given detector geometry and region of interest. The lightly shaded regions of Figure 1 show two natural pixels. Note that unlike the Galerkin basis, the NP basis functions are only orthogonal at a single observing location, otherwise they overlap (as indicated by the darker shaded region).

The measurements  $y_i$  can be written

$$y_i = \int_{\Omega} f(\mathbf{r}) \phi_i(\mathbf{r}) d\mathbf{r} \quad i = 1, \dots, N_t \quad (4)$$

We now construct an estimate of the field  $\hat{f}_{NP}$  as a linear combination in this basis

$$\hat{f}_{NP}(\mathbf{r}) = \sum_{j=1}^{N_t} x_j \cdot \phi_j(\mathbf{r}) \quad (5)$$

where the  $x_j$  are the coefficients of the NP basis expansion. Substituting this estimate into (4) we have

$$y_i = \sum_{j=1}^{N_t} x_j \underbrace{\int_{\Omega} \phi_j(\mathbf{r}) \phi_i(\mathbf{r}) d\mathbf{r}}_{C_{ij}} \quad (6)$$

The term over the brace,  $C_{ij}$ , represents the areas of overlap of natural pixel  $i$  with natural pixel  $j$  (e.g., the darker shaded regions of Figure 1 is an off-diagonal element of  $C$ ). If we consider the entire vector of observations, we may write an equivalent matrix equation

$$y = Cy \quad (7)$$

The NP projection matrix  $C$  has dimensions  $(N_t \times N_t)$ . For example, if we have 3 observing stations with 100 measurements each,  $C$  has dimensions  $(300 \times 300)$ . For comparison, consider a modest discretization of  $\Omega$  into a  $(50 \times 50)$  rectangular pixel grid. The projection matrix  $T$  then has dimensions  $(2500 \times 300)$ , more than 8 times the size of  $C$ .

An efficient algorithm for the solution of (7) was proposed by Buoconore et al. in [6], based on an iterative minimum variance estimate. This algorithm proceeds from an initial guess of  $\hat{x}^0 = [0 \dots 0]$  and uses the following successive state approximation to reach the optimal object estimate  $\hat{x}$ .

$$\hat{x}^{k+1} = \left( I - \frac{1}{N_p} D^{-1} C \right) \hat{x}^k + \frac{1}{N_p} D^{-1} y \quad (8)$$

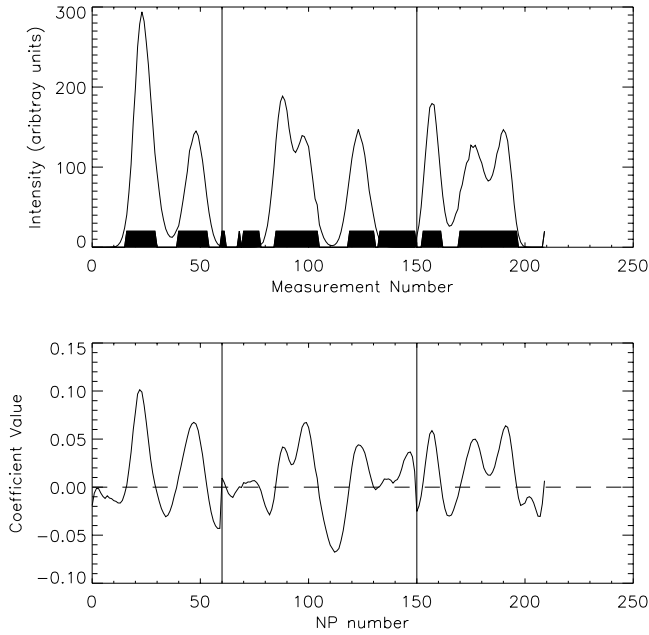


Figure 2: A plot of the data created from the phantom shown in Figure 3a (top panel) along with the corresponding NP coefficients (lower panel). The black bars indicate regions in the data where the NP coefficients are positive. Note that positive coefficients correspond to data maxima.

where

$$D = \text{diag}[C_{ii}] \quad (9)$$

The suboptimal estimates are represented by the state variables associated with the natural pixels instead of those associated with the rectangular pixels, as traditionally used. The algorithm is convergent in the least squares sense

With this solution, we may calculate  $\hat{f}_{NP}$  as follows. Note that the elements of  $C$  are the areas of overlap of the various fan beams, i.e., the inner products of the rows of the rectangular pixel basis  $T$ . With a sufficiently fine rectangular pixelization,  $C$  may be estimated as  $C \approx TT^T$ . Combining this with (7) and (2) results in the relationship between the NP coefficients and the estimated field.

$$\hat{f}_{NP} = T^T \hat{x} \quad (10)$$

Note that this is identically the standard backprojection operation.

As an example, consider the auroral phantom shown in Figure 3a, with a normalized peak density (or photon volume emission) of 1. This structure is observed from 3 stations in the configuration of Figure 1, resulting in

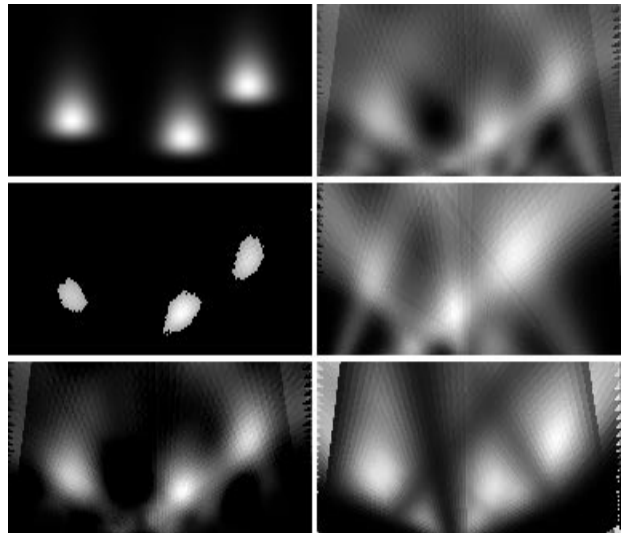


Figure 3: Example NP reconstruction for ionospheric tomography. From left to right, top to bottom: (a) Phantom ionospheric structure ( $f_{\max} = 1.$ ); (b) The NP solution  $\hat{f}_{NP}$ ; (c)  $\hat{f}_{NP}u(\hat{f}_{NP} - .4)$ ; (d) The back-projection solution  $T^T y$ ; (e) The result of refining  $\hat{f}_{NP}$  with entropy regularization; (f) Comparison with MART solution after the same number of iterations.

the projection data shown in the top panel of Figure 2. The cameras have fields of view of  $60^\circ$ ,  $90^\circ$ , and  $60^\circ$  respectively and data are recorded at  $1^\circ$  resolution.

Figure 3b shows  $\hat{f}_{NP}$  after only 5 iterations of (8). The visually displeasing background is due to negative elements in the estimated field. However one can see that the basic morphology of the 3 structures is estimated reasonably well in the NP basis. In fact if we can apply some known limits of occurrence to the reconstructed field, we can isolate the position of the peaks of the phantom structures. As an example, Figure 3c shows the field  $\hat{f}_{NP}u(\hat{f}_{NP} - .4)$  where  $u$  is the unit step function.

For comparison, we show in Figure 3d the back-projection solution  $\hat{f}_{BP} = T^T y$ . Simple backprojection fails to locate accurately the 3 maxima as well as introducing a variety of significant artifacts.

#### 4. IMPROVED SOLUTION USING ENTROPY REGULARIZATION

Due to the very limited number of observations, there may be significant negative values in  $\hat{f}_{NP}$ . Previous works on NP tomography have not addressed this issue, either because the angular coverage used did not

result in any significant negative field estimates or because they were concerned mostly with morphological features of the reconstruction. However, solution positivity constitutes valuable prior information. Indeed, in CIT we are often interested in the absolute magnitudes of the field parameters.

We now use an entropy regularization algorithm to redistribute the energy associated with the negative pixels. Maximum entropy algorithms can be treated in the context of Tikhonov regularization. The object that is optimized can be written as

$$\hat{f} = \operatorname{argmin}_f \{ \|y - Tf\|_2 - \Lambda \|Lf\|_2 \} \quad (11)$$

where the operator  $L$  measures the entropy of  $f$ . Setting  $\Lambda > 0$  means we are prepared to trade off the minimum residual norm solution for one which is positive. There are a variety of multiplicative algorithms developed based on (11). We will here use the parallel log-entropy MART (PLogMART) algorithm proposed by Depierro [7]. PLogMART maximizes the Berg entropy,  $-\ln f$ , subject to  $y = Tf$ .

We must first construct an optimal positive version of  $\hat{f}_{NP}$  to use as the initial guess to PLogMART. However we wish to do this in a way that retains altitude information recovered by the NP estimate. The lower panel of Figure 2 plots the NP coefficient vector  $x$ . The dark bars in the top panel indicate regions of that data where the corresponding NP coefficients are positive. One can see that positive NP coefficients correspond to data maxima. Therefore, removing the negative values in  $\hat{f}_{NP}$  will have the largest effect on the smaller data numbers. As a first guess to our entropy regularization algorithm we may use

$$\hat{f}^0 = \hat{f}_{NP} u(\hat{f}_{NP}) \quad (12)$$

This estimate retains the kernel features in  $\hat{f}_{NP}$ . The final estimate  $\hat{f}$  is shown in Figure 3e. The solution is improved over the NP solution. For comparison, we show in Figure 3e the solution obtained from PLogMART with a constant initial guess after the same number of steps. We note that this solution will eventually converge to the solution in Figure 3d but at greater computational cost.

The steps used to create the above example may be summarized in the following NP algorithm for CIT:

1. For a given detector configuration and region of interest, calculate the natural pixel projection matrix  $C = TT^T$ .
2. Solve  $y = Cx$  for the NP coefficient vector  $\hat{x}$ .
3. Backproject  $\hat{x}$  to obtain  $\hat{f}_{NP} = T^T \hat{x}$ .
4. create  $\hat{f}^0 = \hat{f}_{NP} u(\hat{f}_{NP})$ , and use as initial guess to PLogMART to solve  $y = Tf$ .

## 5. SUMMARY

We have developed a framework for using a natural pixel (NP) decomposition in computerized ionospheric tomography. The NP basis is closely connected to the measurement geometry, and as such provides a measure of the optimal tomographic resolution supported by the data. We have shown by example some advantages that the NP approach offers over standard iterative techniques applied to CIT. The essential features of an ionospheric phantom were recovered at considerably less computation time. We have also addressed the problem of negative elements appearing in fields estimated from an NP basis with very few projections. We have proposed a technique for redistributing this negative energy using an entropy regularization algorithm. We have summarized these technique in a general algorithm that may be applied to any limited angle tomography problem.

## 6. REFERENCES

- [1] Sutton, E. and H. Na, "Ionospheric tomography using the residual correction method", *Radio Sci.*, Vol. 31, No. 3, pp. 489, 1996.
- [2] Fremouw, E.J., J.A. Secan, and B.M. Howe, Application of stochastic inverse theory to ionospheric tomography, *Radion Sci.*, Vol. 27, No. 5, pp. 721-732, 1992.
- [3] Doe, R.A, J.D. Kelly, J.L. Semeter, and D.P. Steele, Tomographic reconstruction of 630.0 nm emission structure for a polar cap arc, *Geophys. Res. Lett.*, Vol. 24, No. 9, pp. 1119, 1997.
- [4] Semeter, J., and Mendillo, M., A nonlinear optimization technique for ground-based atmospheric emission tomography, *IEEE Trans. Geosci. Remote Sensing*, Vol. 35, No. 5, pp. 1105-1116, 1997.
- [5] Bhatia, M., W. C. Karl and A. S. Willsky, "Tomographic reconstruction and estimation based on multiscale natural-pixel bases", *IEEE Transactions on Image Processing*, Vol. 6, No. 3, pp. 463, 1997.
- [6] Buonocore, M. H., W. R. Brody and A. Macovski, A natural pixel decomposition for two dimensional image reconstruction, *IEEE Transactions on Biomedical Engineering*, Vol. BME-28, No. 2, February 1981, pp. 69-78.
- [7] De Pierro, A., Multiplicative iterative methods in computed tomography, in *Mathematical Methods in Tomography*, edited by G.T. Herman, A.K. Louis and F. Natterer, Springer-Verlag, Berlin: 1991.